Research Square

Preprints are preliminary reports that have not undergone peer review.
They should not be considered conclusive, used to inform clinical practice,
or referenced by the media as validated information.

Effect mono-ADP-ribosylation on lipid metabolism of colorectal cancer by regulating IGFBP1 methylation

ChuanLing Wang
School of Basic Medicine, Chongqing Medical University
Yi Tang
School of Basic Medicine, Chongqing Medical University
ShuXian Zhang
School of Basic Medicine, Chongqing Medical University
Ming Xiao
School of Basic Medicine, Chongqing Medical University
Ming Li
School of Basic Medicine, Chongqing Medical University
Lian Yang
School of Basic Medicine, Chongqing Medical University
QingShu Li
School of Basic Medicine, Chongqing Medical University
Xian Li
School of Basic Medicine, Chongqing Medical University
YaLan Wang (wangyalan@cqmu.edu.cn)
School of Basic Medicine, Chongqing Medical University

Research Article

Keywords: MARylation, Histone3, IGFBP1, Lipid metabolism, Methylation, IGF-1R

Posted Date: May 17th, 2023

DOI: https://doi.org/10.21203/rs.3.rs-2935933/v1

License: This work is licensed under a Creative Commons Attribution 4.0 International License.
Read Full License

Abstract

In the global health community, colon cancer (CRC) is a major concern, with a high rate of incidence. Epigenetics is recognized as one of the causes of CRC development and progression. Mono-ADP-ribosylation (MARylation) is a type of epigenetics, although the modification level and the target protein in CRC remain unclear. We previously reported that the MARylation of arginine-117 of histone 3 (H3R117) promotes the proliferation, upregulates methylation of tumor suppressor gene, and is tightly associated with the metabolic processes in LoVo cells. Lipid metabolism disorder is involved in the development of CRC at the early stage. Our study revealed that MARylation of H3R117 of the LoVo cells modulated lipid metabolism, increased cholesterol synthesis, promoted lipid raft (LR) protein IGF-1R distribution, and inhibited cell apoptosis through IGFBP1. In addition, bioinformatics analyses revealed that the IGFBP1 promoter was hypermethylated in CRC when compared to that in normal tissues. Moreover, H3R117 MARylation upregulated the methylation of IGFBP1 promoter through histone H3 citrullination (H3cit) by increasing the H3K9me2, heterochromatin protein1 (HP1), and DNA methyltransferase 1 (DNMT1) enrichment of IGFBP1 promoter. Accordingly, IGFBP1 may function as a tumor suppressor gene, while H3R117 MARylation may promote CRC development. Our study findings enrich the available data on epigenetics of CRC and provide a new idea and experimental basis for H3R117 MARylation as a target in CRC treatment.

1. Introduction

Statistically, CRC ranked third in the rate of incidence (10%) and second in mortality (9.4%) in 2020, making it remains a leading killer worldwide despite the increasing number of anticancer therapies being developed [1, 2]. Considering that CRC is synonymous with a heavy societal and economic burden to the patients and society at large, the underlying mechanisms and treatments of CRC remain to be determined.

The importance of epigenetic abnormalities in tumors is well recognized. MARylation, a single unit of ADP-ribose transferred from NAD^+ to targets, is a type of epigenetics that regulates numerous cellular processes like inflammation, DNA damage repair, and apoptosis [3, 4]. However, the enzymes and targets of MARylation in CRC are unclear. Our past study showed that H3R117 had MARylation, which promotes proliferation, invasion, metastasis and upregulates the mRNA expression of sterol regulatory element-binding transcription factor 1 (SREBP1) and fatty acid synthase (FASN)[5–8], suggesting that MARylation of H3R117 may be related to lipid metabolism in CRC cells. Interestingly, the literature has shown that MARylation is involved in intracellular lipid droplets and fatty acid efflux[9]. Therefore, further research is needed on the role of MARylation in CRC.

Accumulating evidence suggests that lipid metabolism disorder is associated with CRC[10, 11], although the specific mechanism remains unclear. Cancer cells can upregulate endogenous adipogenesis and cholesterol synthesis to meet the needs of tumor growth, and limiting lipid accumulation may be a strategy against malignant tumors. Past studies have demonstrated that FASN, acetyl-CoA carboxylase

(ACC), and 3-hydroxy-3-methylglutaryl-CoA reductase (HMGCR) are the key rate-limiting enzymes for cholesterol and fatty acid synthesis, which are regulated by sterol regulatory element-binding proteins (SREBPs) [11–13]. In addition, the insulin growth factor-1 (IGF-1) and IGF-1 receptor (IGF-1R) can upregulate the transcription of SREBP1, which promote the expression of HMGCR, but the use of IGF-1R inhibitor reverses the above outcome[14–17], suggesting that IGF-1/IGF-1R/SREBP1 play a role in the regulation of fatty acid and cholesterol biosynthesis.

Cholesterol is a key component of the LR in the cell membranes that affect the function of LR-associated proteins, such as protein trafficking and different cellular signaling[18]. Past research has shown that the translocation of IGF-1R to LRs antagonizes drug-induced tumor apoptosis[19]. Moreover, Maryse et al.[20] confirmed that cholesterol depletion destroys the LR stability, prompting the transfer of IGF-1R from LR to non-LR structures and eliminating the apoptosis mediated by IGF-I; however, the addition of cholesterol can reverse the abovementioned results, which implies that cholesterol affects the distribution of IGF-1R on LRs, followed by apoptosis of the cancer cells.

Importantly, the binding of IGF-1 to IGF-1R is regulated by insulin-like growth factor binding protein 1 (IGFBP1). IGFBP1 belongs to the IGF-signaling pathways, which binds IGF-1 with a high affinity and controls its biological activity[21]. IGFBP1 plays an anti-tumor role. According to the literature, the lower the level of IGFBP1, the higher is the risk of CRC [22, 23]. Recently, different studies showed that the abnormal methylation of IGFBP1 is an important factor in gastric cancer[24, 25] and renal cancer[26], but whether it is abnormal in CRC remains unknown. Our studies have demonstrated that the MARylation of H3R117 regulates histone modification and DNA methylation, which in turn affects the tumor suppressor gene expression. Accordingly, we speculated that the MARylation of H3R117 may affect the IGFBP1 methylation of CRC cells.

Thus, our study explored the potential epigenetic mechanisms of H3R117 MARylation on the methylation of IGFBP1 promoter and its impact on the lipid metabolism and apoptosis through IGFBP1 in CRC cells, which may provide the academic basis for establishing potential therapeutic targets of CRC.

2. Materials and methods

2.1. Cell culture

Prof. Wei-Xue Tang (Chongqing Medical University, Chongqing, China) generously provided human colon adenocarcinoma LoVo cells that were maintained in DMEM (Hyclone, Logan, UT, USA) with 10% fetal bovine serum (Hyclone), 1% penicillin and 1% streptomycin at 37°C under 5% CO_2 atmosphere. The point-mutated H3R117 LoVo cells [arginine at residue 117 of H3 is changed to alanine (Mut-1) and lysine (Mut-2)] and empty vector LoVo cells (Ev) have been constructed [6].

2.2. Primary antibodies, reagents, and animals

The following primary antibodies, reagents, and animals were used in this study: anti-IGF-I receptor (9750, Cell Signaling Technology, MA, USA), anti-histone H3 antibody (4620, Cell Signaling Technology), anti-H3K9me2 (4658, Cell Signaling Technology), anti-H3K9me3 (13969, Cell Signaling Technology), anti-Hp1α (2616, Cell Signaling Technology), anti-DNMT1 antibody (24206-1-AP, Proteitech, Chicago, USA), anti-caspase3 antibody (19677-1-AP, Proteitech), anti-SREBP1 antibody (14088-1-AP, Proteitech), anti-caveolin-1 antibody (16447-1-AP, Proteitech), anti-IGFBP1 antibody (A2981, ABclonal, Wuhan, China), anti-histone H3 (citrulline R2 + R8 + R17) antibody (ab5103, Abcam, MA, USA), and PAD inhibitor Cl-amidine (purity > 95% by HPLC,506282, Sigma-Aldrich, USA). Nude mice were provided by the Experimental Animal Center of the National Bio-industry Base in Chongqing Medical University. Mice were sacrificed via cervical dislocation, and the xenograft tumors quickly extracted and snap frozen in liquid nitrogen, and then stored at − 80°C. The study was conducted in accordance with the Declaration of Helsinki, and approved by the Institutional Ethics Committee of ChongQing Medical University.

2.3. Primer sequences

As follows were the oligonucleotide sequences of primers, which were designed using software developed by NCBI. (Table 1).

Table 1
Primer sequences for quantitative PCR

	Primer orientation	Primer sequence (5' to 3')
IGFBP1 mRNA	forward	GAGCACGGAGATAACTGAGGAGG
	reverse	GAGCCTTCGAGCCATCATAGGT
ACC mRNA	forward	CTGGAGGTGCAGATCTTAGCG
	reverse	ATCTTCTGATGCTGCGTTGTA
ACLY mRNA	forward	TGGGGACCACAAGCAGAAGT
	reverse	CTGTCATAGGCAGAGCGGAGA
FASN mRNA	forward	ATGCGGGACAGAGCAACTACG
	reverse	TCGTTGGTGCTCATCGTCTCC
HMGCR mRNA	forward	TGGCCCAGTTGTGCGTCTTC
	reverse	GCCTCCTTTATCACTGCGAACC
β-ACTIN mRNA	forward	GCCCTAGACTTCGAGCAAGA
	reverse	AGGAAGGAAGGCTGAAGAG
IGF-1R mRNA	forward	TGCTGTATGCCTCTGTGAACCC
	reverse	CCTTCATAGACCATCCCAAACG
SREBP1 mRNA	forward	CACCGTTTCTTCGTGGATGG
	reverse	GGGCTGGGTCACACAGTTCA

2.4. Enzyme-linked immunosorbent assay

LoVo cells were grown in 6-well plates. The cell culture supernatants were collected, and the IGF-1 levels were measured as per the manufacturer's protocol using the human IGF-1 ELISA Kit (MB-0032B, Jiangsu Meibiao Biological Technology Co., China). Then, 1×10^7 cells were collected from each group, after which T-CHO and FA were measured by using the total cholesterol assay kit (A111-1, NanJing JianCheng Bioengineering Institute, China) and human FA ELISA Kit (MB-3730B, Jiangsu Meibiao Biological Technology Co.).

2.5. Western blotting

LR proteins were prepared as per the protocols of the UltraRIPA® kit for LR (F015, Funakoshi, Japan). Nuclear and cytosolic proteins were extracted according to the instructions of the total protein and nucleoplasmic protein extraction kit (Beyotime, China). To detect protein concentrations (Beyotime), the BCA assay method was used. Then, the proteins were separated by SDS-PAGE and electroblotted onto the

polyvinylidene fluoride membrane (Millipore, MA, and USA). Incubated at 4°C overnight with primary antibodies after 2 h of blocking at room temperature, including IGFBP1 (1:500 dilution), cavolin (1:800 dilution), caspase3 (1:1000 dilution), H3cit (1:1000 dilution), IGF-1R (1:1000 dilution), SREBP1 (1:500 dilution), β-actin (1:1000 dilution), and H3 (1:1000 dilution). Secondary antibodies were then incubated for 2 hours at room temperature after washing with TBST. Finally, the chemiluminescence signals were visualized with enhanced chemiluminescence reagents (ECL) from Beyotime and analyzed with Quantity One software from Bio-Rad.

2.6. Quantitative PCR

LoVo cells (3×10^5) were collected in 6-well plates and the total RNA was extracted and reverse transcribed using the CellAmpTM Direct RNA Prep Kit for RT-PCR (Takara, China) and the PrimeScriptTM RT Reagent Kit (Perfect Real Time). Our quantitative PCR was performed with the SYBR® Premix Ex Taq™ II (Takara), and target gene expressions were compared to β-actin.

2.7. Small-interfering RNA (SiRNA) procedures

SiRNA targeting IGFBP1 riboFECT™ CP was purchased from the RiboBio Company. siRNA transfection followed manufacturer's instructions. Briefly, 2×10^5 cells were seeded and transfected with 50 nM (6-well plate) siRNA. After 2 days, the transfected cells were used in the subsequent experiments. The selected siRNA sequence was Si#2 (5-ACAGAGTCGTAGAGAGTTT-3).

2.8. Oil red O staining

Lipid accumulation was observed by Oil Red O staining. Fix LoVo cells in 4% paraformaldehyde for 30 minutes, stain with oil red O solution at 37 ° C for 30 minutes, and then wash three times with 60% isopropanol. Mayers hematoxylin was used to counterstain nuclei for 3 min. Under a light microscope (Olympus Corp., Tokyo, Japan), red-stained lipid droplets were observed.

2.9. Raman imaging

After 48 h of transfection, the DXR2xi Raman Imaging Microscope (Thermo Fisher Scientific, USA) with 780 nM excitation and 24-mW laser power was used for acquiring the Raman maps. The spectrum scanning range was 1000 – 1700 cm^{-1}, the aperture was 50-μm slit, and the measurement regions were 15 μm with 1.0-μm spot size. The scanning time was 1 s, and the number of scans was 12. All operations were performed at room temperature. Analyzing the Raman hyperspectral maps was done with the OMINICS software (Thermo Fisher Scientific).

2.10. Flow cytometric analysis of cell apoptosis

The cells were seeded in 6-well plates. After 2 days of transfection, the floating cells were collected. Immediately after digestion with trypsin (without EDTA) and placement in centrifuge tubes, adherent cells were centrifuged. Cells were stained with Annexin V-FITC and PI to measure apoptosis rates with flow cytometry (Becon Dickinson FACS Calibur, NY, USA).

2.11. Construction of the tumor transplantation model

The Committee for Animal Research of the Chongqing Medical University approved the protocol of animal experiments. Balb/c nude mice (female, 5-week-old) were used in the in vivo animal studies. LoVo cells (1×10^7) in 200 μL of PBS were injected into the right subscapular region of nude mice, followed by monitoring of the subcutaneous tumorigenesis of mice. We sacrificed the mice after 14 days and harvested the transplant subcutaneous sarcomas. Tumor volume was determined using calipers, and by the formula: $V = (\text{length} \times \text{width}^2)/2$. Finally, the transplanted tumor was immediately stored in liquid nitrogen.

2.12. Bioinformatics analyses

The methylation status of the IGFBP1 promoter in CRC and normal tissues was obtained from the Human Disease Methylation Database Version 2.0, which is available at http://biobigdata.hrbmu.edu.cn/diseasemeth/.

2.13. Bisulfite sequencing PCR (BSP)

The genomic DNA of each group was collected from 5×10^6 cells, which were modified with sodium bisulfite and then processed by PCR. The primers used for the specific amplification of IGFBP1 promoter sequences are listed above (Table.1). The PCR products were connected to a pMD18-T cloning vector and then transformed. Subsequently, the transformed cells were screened via blue-white selection. The screenings of positive clones were extracted and sequenced by the Shanghai Sangon Bioengineering Co. Ltd. (Shanghai, China). The sequences of primers were in Table 2.

Table 2
The PCR primer for BSP

	Primer orientation	Primer sequence (5' to 3')
IGFBP1	forward	CAGCTCTCCACTGGAAGGCCA
	reverse	GGTCTTGTTAGCAGTGGAGCCAG

2.14. Chromatin immunoprecipitation (ChIP) assay

As previously described, ChIP-qPCR was conducted[5] using the SimpleChIP Enzymatic Chromatin IP Kit (9004, Cell Signaling Technology). Briefly, 540 μL of 37% formaldehyde solution was added to 20 mL of the medium containing 1×10^7 cells) for crosslinking. Subsequently, the cross-linked chromatin was digested and sheared to approximately 150–900-bp DNA fragments via sonication. The input control was reserved, and the remaining Protein–DNA complexes were obtained with the anti-H3k9me2 (5 μL/IP), anti-H3k9me3 (5 μL/IP), anti-H3cit (5 μL/IP), anti-Hp1α (10 μL/IP), or anti-DNMT1 (10 μL/IP) overnight at 4°C. Normal rabbit IgG (5 μL/IP) was used as the negative control. Following washes and DNA elution, qPCR was performed with primers for the IGFBP1 promoter fragment.

2.15. Cell counting kit-8 (CCK-8) assay

3500 cells were added to a 96-well plate for 6 h. In the final concentrations, 100 μm and 200 μm of Cl-amidine were added [27], respectively. After incubation for 12, 24, and 48 h, 10 μL of the CCK-8 solution (Beijing Tongren Institute of Chemistry, Beijing, China) was added, incubating for 2 h. Finally, the absorbance (optical density, OD) was detected at 450 nm.

2.16. Immunofluorescent Confocal Microscopy

4% Paraformaldehyde was applied for 20 minutes to the LoVo cells after seeding them on 6-well glass slides. We then permeated the cells with 0.5% TritonX-100 for 20 min, followed by 2% goat serum for 30 min. Double labeling was performed with anti-Hp1α (1:200) and anti-DNMT1 (1:200) antibodies overnight at 4°C. The day after, secondary antibodies and the DAPI solution in PBS were added. Finally, the glass slides were washed 5 times with PBS and examined by confocal microscopy (Laser Scanning Confocal Microscope LEICA TCS SP2).

2.17. Methylated DNA immunoprecipitation-quantitative PCR (MeDIP-qPCR)

In order to detect the 5-mC immunoprecipitation of IGFBP1 promoter, EpiQuik Methylated DNA Immunoprecipitation Kit (Epigentek, NY, USA) was used for MeDIP-qPCR. The specific experimental steps were performed as described elsewhere[5] .

2.18. Statistical analysis

We repeated the experiment three times with three replicates. Statistical analyses were performed using the SPSS software version 21.0 (SPSS Inc., Chicago, IL) and GraphPad Prism 8.3.0 (GraphPad Software Inc., CA, USA). Data were expressed as mean ± standard deviation ($x \pm s$). The comparisons of groups were computed using a one-way analysis of variance. $P < 0.05$ was considered to indicate statistical significance.

3. Results

3.1. Effects of MARylation of H3R117 on fatty acids and cholesterol in LoVo cells

For rapid growth, tumor cells can enhance endogenous adipogenesis and cholesterol synthesis. Therefore, ELISA was used to detente the contents of cholesterol and fatty acids, which were significantly lower in mutant groups than those in control and empty vector groups (Figure. 1A-B). Previous experimental results found that the MARylation of H3R117 can promote the mRNA expression of SREBP1 and FASN [8], which may be involved in lipid metabolism. Coincidentally, this result confirms previous speculation.

3.2. Effects of MARylation of H3R117 on the rate-limiting enzymes ACC, ACLY, FASN, and HMGCR *in lipid metabolism of LoVo cells*

Researches have shown that IGF-1 and IGF-1R regulates SREBP1, which in turn affects the rate-limiting enzyme of fatty acid and cholesterol synthesis [15–17, 28]. Moreover, IGFBP1 is the molecular switch of IGF-1. Accordingly, we tested the abovementioned indicators. Compared with empty vector and control group, two mutant groups showed decreased levels of IGF-1 in the culture supernatant (Figure. 1C), increased protein levels of IGFBP1, and reduced protein expression of IGF-1R and SREBP1 (Figure. 1D-E). Additionally, the mRNA levels of ACC, FASN, and HMGCR were significantly lower in mutant groups compared to empty vector and control groups, although no significant difference in ACLY was noted (Figure. 1F). These results suggest that MARylation of H3R117 was involved in regulating the rate-limiting enzyme of lipid metabolism in LoVo cells.

3.3. Effects of MARylation of H3R117 on lipid metabolism via IGFBP1 in LoVo cells

To explore the role of IGFBP1 in the lipid metabolism of LoVo cells, we further examined the effects of IGFBP1 by siRNA-mediated IGFBP1 knockdown. The optimal interfering sequence si#2 was determined by qRT-PCR and Western blotting (Figure. 1G-I, Supplementary Figure. 1). When compared with the two mutant groups, after the knockdown of IGFBP1, supernatant levels of IGF-1 grew along with IGF-1R, SREBP1, ACC, FASN, and HMGCR mRNA levels (Figure.1J-K), and the oil red O staining region was upregulated(Figure.1L), suggesting that MARylation of H3R117 may regulate the lipid metabolism through IGFBP1 in LoVo cells.

3.4. Effects of MARylation of H3R117 on cholesterol by IGFBP1 in LoVo cells

The content of cholesterol has an important effect on the fluidity of cell membrane and the distribution of protein on the LRs. So, Raman confocal microscopy was used to measure the cholesterol levels in each group since HMGCR is a key in cholesterol synthesis. The laser Raman spectrum of the cholesterol in the wavenumber of 1000–1700cm-1 was selected. We noted a strong Raman peak at the Raman shift of 1439 cm-1 of the cholesterol standard (Figure. 2A), which was then selected as the Raman intensity comparison. Plainly, when compared with two mutant groups, the Raman intensity increased significantly after knocking down IGFBP1 (Figure. 2B), thereby indicating that MARylation of H3R117 elevated the cholesterol content through IGFBP1 in LoVo cells.

3.5. Effects of MARylation of H3R117 on the expression of IGF-1R in LR, nucleus, and cytoplasm by IGFBP1 in LoVo cells

Cholesterol is a major component of LRs and affects the distribution and function of LR protein. The literature demonstrates IGF-1R can be transferred from the cell membrane LR domains to the nucleus and that its distribution on LR is affected by cholesterol. Therefore, we tested whether MARylation of H3R117 further affects the distribution of IGF-1R in LoVo cells. Our results indicated that the IGF-1R of LR and the nucleus of mutant groups decreased significantly when compared with the empty vector and control groups. When compared with the mutant groups, the IGF-1R of LR and nucleus increased significantly after knocking down IGFBP1 (Figure. 2C-E). This result implies that the MARylation of H3R117 may affect the distribution of IGF-1R in different portions by IGFBP1 in LoVo cells.

3.6. Effects of MARylation of H3R117 on apoptosis by IGFBP1 in LoVo cells

Past literatures have demonstrated that increased distribution of IGF-1R on the LR can inhibit the apoptosis of cancer through different pathways. Therefore, the expression of caspase3 was detected by flow cytometry (Figure. 2F-G). In comparison with control and empty vector groups, the mutant groups had higher apoptosis rate. When compared with the mutant groups, the apoptosis rate decreased after knocking down IGFBP1, thereby suggesting that H3R117 MARylation may inhibit apoptosis through IGFBP1 in LoVo cells.

3.7. Effects of MARylation of H3R117 on the expression of IGFBP1, IGF-1R, SREBP1, and Caspase3 in subcutaneous transplanted tumors

Previously, we transplanted LoVo cells of four groups subcutaneously into nude mice and found that transplanted tumors in mutant groups were smaller in weight and volume than those in control groups in the control and empty vector groups[6]. Meanwhile, consistent results were obtained in this experiment (Figure. 3A-B). Moreover, when compared with empty vector and control groups, the IGFBP1 and cleaved caspase3 expression in the mutation groups increased, while IGF-1R and SREBP1 decreased (Figure. 3C-D). Thus, these in vivo data are consistent with those of the above-mentioned in vitro experiments.

3.8. IGFBP1 promoter methylation analysis in CRC tissues by bioinformatics

Based on the above-mentioned results, the MARylation of H3R117 in LoVo cells can affect lipid metabolism and inhibit apoptosis through IGFBP1, albeit the specific mechanism underlying this phenomenon is unclear. Recent studies revealed that abnormal IGFBP1 methylation is an important factor in cancer development[24, 25]. However, the methylation status of IGFBP1 in CRC continues to remain unclear. Therefore, we detected the promoter methylation of IGFBP1 in CRC and normal tissues by bioinformatics. The analysis indicated higher levels of methylation at IGFBP1 promoter in CRC than in

normal specimens (Figure.4A-B), which may be one of the reasons for the decreased expression of IGFBP1.

3.9. Effect of MARylation of H3R117 on the IGFBP1 promoter methylation in LoVo cells

Our past studies demonstrated that the MARylation of H3R117 could regulate oncogene promoter methylation[5], and IGFBP1 promoter methylation was higher in CRC than in the normal tissues. Thereby the methylation level of IGFBP1 promoter was detected by BSP in LoVo cells. We found that the methylation level of IGFBP1 promoter was significantly lower in mutants groups than in control and empty vector groups (Figure. 4C-D), which may explain the increase in IGFBP1 after removing MARylation of H3R117 from LoVo cells.

3.10. Effects of MARylation of H3R117 on H3K9me2 and H3K9me3 modifications and HP1 and DNMT1 enrichment on IGFBP1 Promoter in LoVo cells

H3R117 MARylation can affect the H3K9me3 modification on oncogene promoters and regulate gene methylation[5]. Accordingly, we detected changes in methylation of H3K9 on the IGFBP1 promoter in LoVo cells by ChIP-qPCR. Our results revealed the mutant groups were less likely to have enriched H3K9me2 on the IGFBP1 promoter than the control and empty vector groups (Figure. 4E-F), albeit no differences were noted for H3K9me3 (Figure. 4I). In addition, it has been reported that H3K9me2 is the binding site of HP1, which then activates DNMT1 leading to DNA methylation[29, 30]. Our data revealed a significantly decreased HP1 and DNMT1 enrichment on IGFBP1 promoter after removing MARylation of H3R117 (Figure.4G-H), suggesting that the MARylation of H3R117 may increase H3K9me2, HP1, and DNMT1 enrichment, resulting in hypermethylation of the IGFBP1 promoter and decreased IGFBP1 expression in the LoVo cells.

3.11. Effects of MARylation of H3R117 on the IGFBP1 expression by H3 citrullination in LoVo cells

Considering the combination of H3K9me2 and HP1, recruiting DNMT1 may be the main step of increased methylation of the IGFBP1 promoter. The literatures demonstrate that histone H3 citrullination (H3cit) inhibits H3K9 methylation and reduces the affinity between H3K9me2 and HP1 [29, 31]. Moreover, Young et al.[32] claimed that the inhibition of H3cit by Cl-amidine decreased the IGFBP1 expression. Therefore, we speculated that H3cit was deeply related to IGFBP1. Our results revealed that the MARylation of H3R117 suppressed the H3cit expression (Figure. 5A-B) and the enrichment of H3cit on the IGFBP1 promoter (Figure. 5C-D). Next, the time and concentration of inhibitor Cl-amidine was selected by CCK-8 for 48 h and 200 μm (Figure. 5E). When compared with the mutant groups, H3cit and IGFBP1 expression

decreased significantly after adding Cl-amidine (Figure. 5F), suggesting that MARylation of H3R117 may regulate the IGFBP1 expression by H3cit in LoVo cells.

3.12. Effect of inhibitor Cl-amidine on the co-localization of HP1 and DNMT1 and the methylation of IGFBP1 promoter in LoVo cells

Based on the above results, we noted increased methylation levels of IGFBP1 promoter in the control and empty vector groups, which was regulated by MARylation of H3R117 affected by H3cit in LoVo cells. Notably, H3cit mainly affected the enrichment of H3K9me2, HP1, and DNMT1 on IGFBP1 promoter. Hence, the co-localization between HP1 and DNMT1 was detected by confocal fluorescence microscopy. The observation indicated an increase in the yellow (merge) co-localization of HP1 (green) and DNMT1 (red) after adding Cl-amidine (Figure. 5G). In addition, the methylation level of the IGFBP1 promoter detected by MeDIP-qPCR showed a corresponding increase after the addition of Cl-amidine (Figure. 5H-I).

4. Discussion

MARylation is believed to be related to signal transduction, stress response, and DNA damage repair [33–35], which are the main pathophysiological mechanisms of the occurrence and development of CRC. Although it is known that the effect of MARylation depends on the specific targets of its modification, its function has not been well-studied owing to technical limitations. Previously, we analyzed the MARylation sites of histone 3 in CRC cell lines by LC-MS/MS and found that H3R117 MARylation in LoVo cells may promote tumor proliferation[6]. Then, we applied the transcriptome sequencing technology to analyze the function of MARylation of H3R117 after the mutation of arginine-117, which indicated that the MARylation of H3R117 may facilitate tumor metastasis and regulate the metabolism processes, such as the lipid metabolic process [8]. However, the mechanism by which MARylation of H3R117 in LoVo cells regulates lipid metabolism remains unknown.

Lipid metabolism disorders are a major feature of tumors to meet the needs of their rapid division, and despite the sufficient level of exogenous fatty acids, tumors tend to synthesize themselves[36, 37]. Past studies have demonstrated that FASN, ACC, and HMGCR are the key rate-limiting enzymes for cholesterol and fatty acid synthesis, which are regulated by SREBPs. Moreover, the combination of IGF-1 and IGF-1R can upregulate the transcription of SREBP1[11, 13, 38], leading to lipogenesis; increasing IGF-1 can promote the expression of HMGCR, but the application of IGF-1R inhibitor reverses these results[14, 17], suggesting the involvement of IGF-1/IGF-1R/SREBP1 in the regulation of fatty acid and cholesterol biosynthesis. However, IGFBP1 is the key regulating factor in the binding of IGF-1 and IGF-1R. Published literature confirms that the main function of IGFBP1 is to strongly bind to IGF and inhibit IGF activity[39]. In other words, up-regulating IGFBP1 reduces the amount of IGF-1 that can interact with IGF-1R. Here, we demonstrated that H3R117 MARylation increased the synthesis of fatty acids and cholesterol, decreased the expression of IGFBP1, upregulated the level of IGF-1 in the supernatant, and enhanced the expression of IGF-1R and SREBP1 as well as those of the downstream ACC, FASN, and HMGCR in LoVo cells. These

results further prove that the H3R117 MARylation participates in the regulation of LoVo cells' cholesterol and fatty acid synthesis, which conforms to the results of a previous study [8] .

Cholesterol is a critical component for the LRs in cell membranes affecting the function of LR-associated proteins [18, 40]. Research implicates that IGF-1R on the cell membrane can be transferred to the nucleus by endocytosis relating to its function[41]. For example, the translocation of IGF-1R to LRs antagonize drug-induced tumor apoptosis[19]. Moreover, Maryse et al.[20] confirmed that cholesterol depletion destroyed the LR stability, causing the transfer of IGF-1R from LR to non-LR structures and eliminating the apoptosis mediated by IGF-I; however, the addition of cholesterol actually reversed the above results, indicating that cholesterol affected the distribution of IGF-1R on LRs, followed by apoptosis of the cancer cells. Subsequently, the content of cholesterol in the LoVo cells was detected by Raman confocal microscopy. These results showed that the MARylation of H3R117 could increase cholesterol synthesis in LoVo cells by IGFBP1. Then, we found that H3R117 MARylation upregulated the expression of IGF-1R in LR and nucleus, accompanied by reduced apoptosis after knocking down IGFBP1 in LoVo cells. In vivo, the volume of subcutaneous xenograft tumors with the MARylation of H3R117 in nude mice was larger than that without, while IGFBP1 and cleavage caspase3 expression decreased along with an increased expression of IGF-1R and SREBP1; the results in vitro were in line with previous fingdings [6]. These results suggest that H3R117 MARylation in LoVo cells may accelerate cholesterol synthesis such that the IGF-1R expression in LR increases and then inhibits apoptosis through IGFBP1 toward promoting the development of CRC.

Based on the appeal results, IGFBP1 was determined to be the key molecule for MARylation of H3R117 toward regulating the malignant tumor behavior, but how IGFBP1 is manipulated remains unclear. The studies suggest that IGFBP1 exerted an antitumor effect in CRC; the risk of CRC was higher with a decrease in the IGFBP1 [22, 23]. Recently, literature suggests that the abnormal methylation of IGFBP1 is an important factor in gastric cancer[24], diabetes[42], and renal cancer[26, 43]. Interestingly, we applied bioinformatics analysis to demonstrate that the methylation of IGFBP1 promoter in CRC was significantly higher than that in the normal tissues, while BSP results showed the MARylation of H3R117 enhanced the IGFBP1 promoter methylation in LoVo cells, which further confirmed the importance of IGFBP1 methylation in CRC. Furthermore, the MARylation of H3R117 may decrease the IGFBP1 expression by promoting the methylation of IGFBP1.

It is already known that histone modification interacts with DNA methylation; H3K9 methylation is widely assumed to be a marker of epigenetic silencing [44–46], which involves the regulation of demethylation and methylation of oncogenes and tumor suppressor genes. Coincidentally, our past studies have shown that the MARylation of H3R117 promoted the expression of H3K9me2 and regulated the methylation of the promoters H3K9, H3K4, and H3K27 at the tumor suppressor gene promoter, thereby increasing the DNA methylation and inhibiting the gene expression[5]. In this study, the MARylation of H3R117 increased the H3K9me2 at the IGFBP1 promoter rather than that of the H3K9me3 in LoVo cells. H3K9me2, a repressive chromatin modification, provides a binding site for HP1, leading to the formation of a silent chromatin state [47–49]. Moreover, HP1 can activate the activity of DNMT1, which co-localizes with HP1

at the H3K9me2 sites, leading to the methylation of cytosine [30, 49, 50]. For instance, altering the H3K9me2 modification level and the recruitment of transcription factors HP1 and DNMT1 in the gene promoter region can inhibit the metastasis of lung cancer [51], suggesting that H3K9me2, HP1, and DNMT1 restrict each other when regulating gene methylation. Correspondingly, our results revealed that H3R117 MARylation increases the enrichment of HP1 and DNMT1 at the IGFBP1 promoter regions in LoVo cells, implying that the MARylation of H3R117 may repress the transcription of IGFBP1 by regulating the binding of H3K9me2, HP1, and DNMT1 on the IGFBP1 promoter.

Since the binding of H3K9me2 to HP1 may be the main step in controlling methylation, we further explored how the MARylation of H3R117 affects the binding of H3K9me2 to HP1. Citrullination is an irreversible PTM that catalyzes the conversion of arginine residues to citrulline, detected in inflammation, autoimmune diseases, and tumors[52, 53]. Past studies have demonstrated negative crosstalk between histone methylation and citrullination; for example, Clancy et al. suggested that the methylation of histone 3 lysine 27 (H3K27) inhibits the citrullination of histone 3 arginine 26 (H3R26) by 30-fold, while the citrullination of H3R26 inhibits the methylation of H3K27 by 30000-fold[31]. In addition, inhibition of citrullination by Cl-amidine resulted in a significant decrease in the IGFBP1 expression [32, 54], which in turn prompted histone citrullination leading to the modulation of the combination of epigenetic modifications at the IGFBP1 promoter sequence. Accordingly, our results suggested that the removal of H3R117 MARylation increased the expression of H3cit and its level at the IGFBP1 promoter regions in LoVo cells. Adding inhibitor Cl-amidine, the expression of H3cit and IGFBP1 decreased as well, indicating that the MARylation of H3R117 may regulate the IGFBP1 methylation and expression by affecting H3cit in LoVo cells.

Thus, we speculated that the MARylation of H3R117 may interfere with the enrichment of HP1 and DNMT1 on the IGFBP1 promoter by affecting H3cit and then H3K9me2. H3cit is believed to inhibit the expression of HP1 and reduce its affinity for H3K9 methylation [29, 31, 55], which may further affect the enrichment of DNMT1 on the gene promoter. Therefore, we examined the co-localization of HP1 with DNMT1 in LoVo cells by laser confocal microscopy and found that Cl-amidine treatment of LoVo cells increased the co-localization with HP1 and DNMT1. Consistently, DNA methylation levels of IGFBP1 promoter detected by MeDIP-qPCR suggested a significant increase after the addition of Cl-amidine, indicating that the MARylation of H3R117 increased the IGFBP1 promoter methylation by regulating histone citrullination.

In conclusion, we showed here that H3R117 MARylation in LoVo cells can simultaneously decrease the level of H3cit, increase the level of H3K9me2, and facilitate cytosine methylation by histone citrullination, which together enhances the binding of HP1 and DNMT1 on the IGFBP1 promoter, thereby inhibiting its expression. Furthermore, the MARylation of H3R117 notably enhanced cholesterol synthesis by IGFBP1, which increased the distribution of IGF-1R in LR, resulting in decreased apoptosis (Figure. 6). In summary, the results in this paper establish the role of H3R117 MARylation in regulating the epigenetic events, modulating lipid metabolism, and inhibiting tumor apoptosis in colon cancer, which promotes the development of CRC. However, there are still some shortcomings in this study. In the early stage, we

screened two cells with higher expression of MARylation in three human colorectal cancer cells (SW480, LoVo, HT29) (Supplementary Fig. 1), and continued to analyze the MARylation at arginine of histone in SW480 and LoVo cells with LC-MS/MS. It was found that only LoVo cells with the highest malignancy had MARylation at H3R117, so the function of H3R117 MARylation cannot be tested in different cell lines at present. We plan to detect the H3R117 MARylation in cancer tissues with different degrees of differentiation from colorectal cancer patients to observe whether H3R117 MARylation can be used to as a molecular target of tumor treatment.

Abbreviations

CRC, colon cancer; MARylation, Mono-ADP-ribosylation; H3R117, arginine-117 of histone 3; LR, lipid raft; H3cit, histone H3 citrullination; HP1, heterochromatin protein1; DNMT1, DNA methyltransferase 1; SREBP1, sterol regulatory element-binding transcription factor 1; FASN, fatty acid synthase; ACC, acetyl-CoA carboxylase; HMGCR, 3-hydroxy-3-methylglutaryl-CoA reductase; IGF-1, insulin growth factor-1; IGF-1R, IGF-1 receptor; IGFBP1, insulin-like growth factor binding protein 1; ACLY, ATP citrate lyase.

Declarations

Data availability

All data are contained within the article.

Declaration of Interest

The authors declare no conflict of interest.

CRediT author contribution

Conceptualization, C. W. and Y. T.; data curation, S. Z.; writing—original draft preparation, C. W.; writing—review and editing, M. X. and X. L.; supervision, Q. L.; project administration, L. Y.; funding acquisition, M. L and Y. W. All authors have read and agreed to the published version of the manuscript.

Acknowledgments

This research was funded by Innovation Project of Graduate Students in Chongqing (grant no. CYB17100); Scientific and Technological Research Program of Chongqing Municipal Education Commission (grant no. KJQN201900403).

References

1. Sung, H., et al., *Global cancer statistics 2020: GLOBOCAN estimates of incidence and mortality worldwide for 36 cancers in 185 countries.* CA: a cancer journal for clinicians, 2021. **71**(3): p. 209-249.

2. Xia, C., et al., *Cancer statistics in China and United States, 2022: profiles, trends, and determinants.* Chin Med J (Engl), 2022. **135**(5): p. 584-590.
3. Kraus, W., *PARPs and ADP-ribosylation: 60 years on.* Genes Dev, 2020: p. 251-253.
4. Lüscher, B., et al., *ADP-ribosyltransferases, an update on function and nomenclature.* FEBS J, 2021.
5. Li, M., et al., *Mono-ADP-ribosylation of H3R117 traps 5mC hydroxylase TET1 to impair demethylation of tumor suppressor gene TFPI2.* Oncogene, 2019. **38**(18): p. 3488-3503.
6. Ling, F., et al., *Mono-ADP-ribosylation of histone 3 at arginine-117 promotes proliferation through its interaction with P300.* Oncotarget, 2017. **8**(42): p. 72773-72787.
7. Wang, C.L., et al., *Analysis of Mono-ADP-Ribosylation Levels in Human Colorectal Cancer.* Cancer Manag Res, 2021. **13**: p. 2401-2409.
8. Zhang, N.N., et al., *Transcriptome sequencing analysis of mono-ADP-ribosylation in colorectal cancer cells.* Oncol Rep, 2020. **43**(5): p. 1413-1428.
9. Bartz, R., et al., *Evidence that mono-ADP-ribosylation of CtBP1/BARS regulates lipid storage.* Mol Biol Cell, 2007. **18**(8): p. 3015-25.
10. Krauß, D., O. Fari, and M. Sibilia, *Lipid Metabolism Interplay in CRC—An Update.* Metabolites, 2022. **12**(3): p. 213.
11. Zaytseva, Y., *Lipid metabolism as a targetable metabolic vulnerability in colorectal cancer*. 2021, Multidisciplinary Digital Publishing Institute. p. 301.
12. Bai, X., et al., *Inhibition of SREBP-mediated lipid biosynthesis and activation of multiple anticancer mechanisms by platinum complexes: Ascribe possibilities of new antitumor strategies.* Eur J Med Chem, 2022. **227**: p. 113920.
13. Wen, Y.A., et al., *Downregulation of SREBP inhibits tumor growth and initiation by altering cellular metabolism in colon cancer.* Cell Death Dis, 2018. **9**(3): p. 265.
14. Johnson, C., J. Kastelic, and J. Thundathil, *Role of Akt and mammalian target of rapamycin signalling in insulin-like growth factor 1-mediated cell proliferation in porcine Sertoli cells.* Reprod Fertil Dev, 2020. **32**(10): p. 929-940.
15. Bhasker, C.R. and T. Friedmann, *Insulin-like growth factor-1 coordinately induces the expression of fatty acid and cholesterol biosynthetic genes in murine C2C12 myoblasts.* BMC Genomics, 2008. **9**: p. 535.
16. Kwon, H.H., et al., *Activity-guided purification identifies lupeol, a pentacyclic triterpene, as a therapeutic agent multiple pathogenic factors of acne.* J Invest Dermatol, 2015. **135**(6): p. 1491-1500.
17. Smith, T.M., et al., *IGF-1 induces SREBP-1 expression and lipogenesis in SEB-1 sebocytes via activation of the phosphoinositide 3-kinase/Akt pathway.* J Invest Dermatol, 2008. **128**(5): p. 1286-93.
18. Vona, R., E. Iessi, and P. Matarrese, *Role of cholesterol and lipid rafts in cancer signaling. A promising therapeutic opportunity?* Front Cell Dev Biol. , 2021. **9**: p. 468.

19. Xu, L., et al., *Oxaliplatin enhances TRAIL-induced apoptosis in gastric cancer cells by CBL-regulated death receptor redistribution in lipid rafts.* FEBS Lett, 2009. **583**(5): p. 943-8.
20. Remacle-Bonnet, M., et al., *Membrane rafts segregate pro- from anti-apoptotic insulin-like growth factor-I receptor signaling in colon carcinoma cells stimulated by members of the tumor necrosis factor superfamily.* Am J Pathol. , 2005. **167**(3): p. 761-73.
21. Lin, Y.-W., et al., *IGFBP-1 in cancer: expression, molecular mechanisms, and potential clinical implications.* Am J Transl Res, 2021. **13**(3): p. 813.
22. Wei, E., et al., *A prospective study of C-peptide, insulin-like growth factor-I, insulin-like growth factor binding protein-1, and the risk of colorectal cancer in women.* Cancer Epidemiol Biomarkers Prev, 2005. **14**(4): p. 850-5.
23. Hang, D., et al., *Plasma Biomarkers of Insulin and the Insulin-like Growth Factor Axis, and Risk of Colorectal Adenoma and Serrated Polyp.* JNCI Cancer Spectr, 2019. **3**(3): p. pkz056.
24. Liang, Y., C. Zhang, and D. Dai, *Identification of DNA methylation-regulated differentially-expressed genes and related pathways using Illumina 450K BeadChip and bioinformatic analysis in gastric cancer.* Pathol Res Pract 2019. **215**(10): p. 152570.
25. Zeng, Z., D. Xie, and J. Gong, *Genome-wide identification of CpG island methylator phenotype related gene signature as a novel prognostic biomarker of gastric cancer.* PeerJ, 2020. **8**: p. e9624.
26. Dzik, C., et al., *Gene expression profile of renal cell carcinomas after neoadjuvant treatment with sunitinib: new pathways revealed.* Int J Biol Markers, 2017. **32**(2): p. e210-e217.
27. Wang, L., et al., *PADI2-Mediated Citrullination Promotes Prostate Cancer Progression.* 2017. **77**(21): p. 5755-5768.
28. Suh, Y., et al., *Platycodin D May Improve Acne and Prevent Scarring by Downregulating SREBP-1 Expression Via Inhibition of IGF-1R/PI3K/Akt Pathway and Modulating Inflammation with an Increase in Collagen.* Ann Dermatol, 2018. **30**(5): p. 581-587.
29. Sharma, P., et al., *Citrullination of histone H3 interferes with HP1-mediated transcriptional repression.* PLoS genetics, 2012. **8**(9): p. e1002934.
30. Smallwood, A., et al., *Functional cooperation between HP1 and DNMT1 mediates gene silencing.* Genes Dev, 2007. **21**(10): p. 1169-78.
31. Clancy, K., et al., *Citrullination/Methylation Crosstalk on Histone H3 Regulates ER-Target Gene Transcription.* ACS Chem Biol, 2017. **12**(6): p. 1691-1702.
32. Young, C., et al., *Progesterone stimulates histone citrullination to increase IGFBP1 expression in uterine cells.* Reproduction, 2021. **162**(2): p. 117-127.
33. Zha, J., Y. Tang, and Y. Wang, *Role of mono-ADP-ribosylation histone modification (Review).* Exp Ther Med, 2021. **21**(6): p. 577.
34. Lüscher, B., et al., *ADP-ribosylation, a multifaceted posttranslational modification involved in the control of cell physiology in health and disease.* Chemical reviews, 2018. **118**(3): p. 1092-1136.

35. Bütepage, M., et al., *Intracellular mono-ADP-ribosylation in signaling and disease.* Cells, 2015. **4**(4): p. 569-595.
36. Butler, L., et al., *Lipids and cancer: Emerging roles in pathogenesis, diagnosis and therapeutic intervention.* Adv Drug Deliv Rev, 2020. **159**: p. 245-293.
37. Broadfield, L., et al., *Lipid metabolism in cancer: New perspectives and emerging mechanisms.* Dev Cell, 2021. **56**(10): p. 1363-1393.
38. Bengoechea-Alonso, M. and J. Ericsson, *SREBP in signal transduction: cholesterol metabolism and beyond.* Curr Opin Cell Biol, 2007. **19**(2): p. 215-22.
39. Baxter, R., *IGF binding proteins in cancer: mechanistic and clinical insights.* Nat Rev Cancer, 2014. **14**(5): p. 329-41.
40. Li, B., et al., *Lipid raft involvement in signal transduction in cancer cell survival, cell death and metastasis.* Cell Prolif, 2022. **55**(1): p. e13167.
41. Aleksic, T., et al., *Type 1 insulin-like growth factor receptor translocates to the nucleus of human tumor cells.* Cancer Res, 2010. **70**(16): p. 6412-9.
42. Gu, T., et al., *Epigenetic analyses of the insulin-like growth factor binding protein 1 gene in type 1 diabetes and diabetic nephropathy.* Clin Epigenetics, 2014. **6**(1): p. 10.
43. Ibanez de Caceres, I., et al., *Identification of novel target genes by an epigenetic reactivation screen of renal cancer.* Cancer Res, 2006. **66**(10): p. 5021-8.
44. Wang, X., et al., *A composite DNA element that functions as a maintainer required for epigenetic inheritance of heterochromatin.* Mol Cell, 2021. **81**(19): p. 3979-3991.e4.
45. Xu, L. and H. Jiang, *Writing and Reading Histone H3 Lysine 9 Methylation in Arabidopsis.* Front Plant Sci, 2020. **11**: p. 452.
46. Zheng, Y., et al., *H3K9me-enhanced DNA hypermethylation of the p16INK4a gene: an epigenetic signature for spontaneous transformation of rat mesenchymal stem cells.* Stem Cells Dev, 2013. **22**(2): p. 256-67.
47. Zhao, S., et al., *Plant HP1 protein ADCP1 links multivalent H3K9 methylation readout to heterochromatin formation.* Cell Res, 2019. **29**(1): p. 54-66.
48. Ryan, D. and D. Tremethick, *The interplay between H2A.Z and H3K9 methylation in regulating HP1α binding to linker histone-containing chromatin.* Nucleic Acids Res, 2018. **46**(18): p. 9353-9366.
49. Honda, S., et al., *Heterochromatin protein 1 forms distinct complexes to direct histone deacetylation and DNA methylation.* Nat Struct Mol Biol, 2012. **19**(5): p. 471-7, S1.
50. Yearim, A., et al., *HP1 is involved in regulating the global impact of DNA methylation on alternative splicing.* Cell Rep, 2015. **10**(7): p. 1122-34.
51. Chen, M., et al., *H3K9 histone methyltransferase G9a promotes lung cancer invasion and metastasis by silencing the cell adhesion molecule Ep-CAM.* Cancer Res 2010. **70**(20): p. 7830-40.
52. Zhu, D., Y. Zhang, and S. Wang, *Histone citrullination: a new target for tumors.* Mol Cancer, 2021. **20**(1): p. 90.

53. Ciesielski, O., et al., *Citrullination in the pathology of inflammatory and autoimmune disorders: recent advances and future perspectives.* Cell Mol Life Sci, 2022. **79**(2): p. 94.
54. Young, C., et al., *Citrullination regulates the expression of insulin-like growth factor-binding protein 1 (IGFBP1) in ovine uterine luminal epithelial cells.* Reproduction, 2017. **153**(1): p. 1-10.
55. Leshner, M., et al., *PAD4 mediated histone hypercitrullination induces heterochromatin decondensation and chromatin unfolding to form neutrophil extracellular trap-like structures.* Front Immunol 2012. **3**: p. 307.

Figures

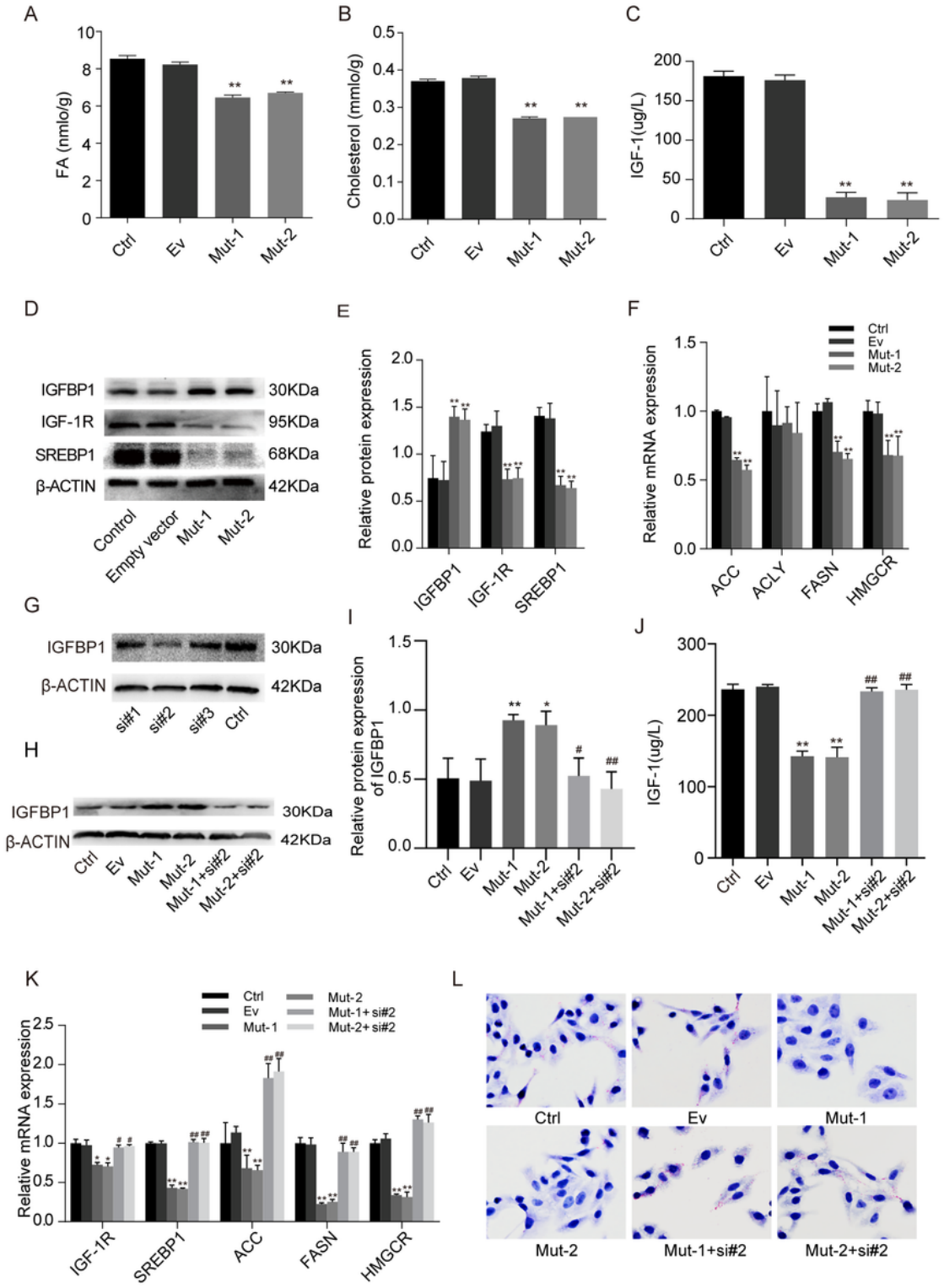

Figure 1

Effect of H3R117 MARylation on lipid metabolism of LoVo cells via IGFBP1. (A-B) The effect of H3R117 MARylation on the levels of fatty acids and cholesterol. The mutant groups had significantly lower levels of fatty acid (A) and cholesterol (B) in comparison with the empty vector group and the control group. **(C-F)** The effect of H3R117 MARylation on the enzymes of lipid metabolism. H3R117 MARylation increased the level of IGF-1 in the supernatant (C) and modified the expression of different proteins (D); Statistical

chart indicating the different protein (E) and mRNA expression (F). **(G-L)** H3R117 MARylation interferes with lipid metabolism through IGFBP1. Effective siRNA sequences were screened by Western blotting analyses (G), the protein expression of IGFBP1 (H-I), the level of IGF-1 in the supernatant (J) and the mRNA expression of different indicators (K) interfered by siRNA. Cells were stained using the Oil Red O to display fat contents (L). (*p < 0.05 vs. Ctrl and Ev; **p < 0.01 vs. Ctrl and Ev; #p < 0.05 vs. Mut-1 and Mut-2; ##p < 0.01 vs. Mut-1 and Mut-2). Abbreviation: Ctrl, Control; Ev, empty vector; Mut-1, arginine at residue 117 of H3 is changed to alanine; Mut-2, arginine at residue 117 of H3 is changed to lysine.

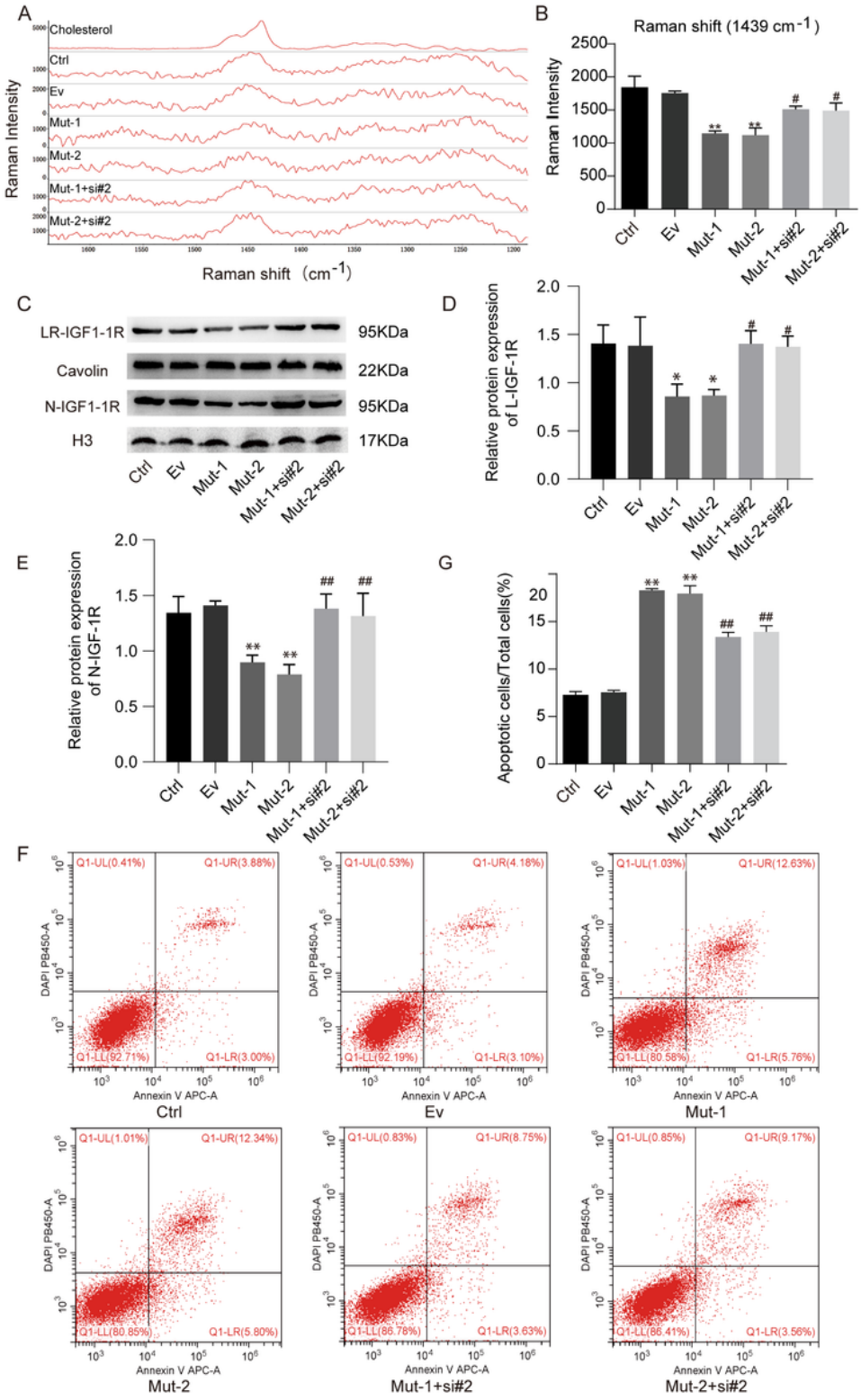

Figure 2

Effect of H3R117 MARylation on cholesterol, and the IGF-1R expression in LR and cell apoptosis by IGFBP1. (A-B) Raman confocal microscopy for cholesterol. The Raman spectra (A) and Raman intensity (B) of cholesterol in different groups. **(C-E)** The effect of H3R117 MARylation on the IGF-1R expression in different parts of LoVo cells via IGFBP1. Western blotting analyses of the IGF-1R expression in LR and nuclei (C); Statistical chart of the IGF-1R protein expression in LR (D) and nucleus (E). **(F-G)** The effect of H3R117 MARylation on apoptosis in LoVo cells by IGFBP1. The flow chart in different groups (F) and statistical chart of apoptosis rate (G). (LR, lipid raft; N, nucleus; **p < 0.01 vs. Ctrl and Ev, ##p < 0.01 vs. Mut-1 and Mut-2 group).

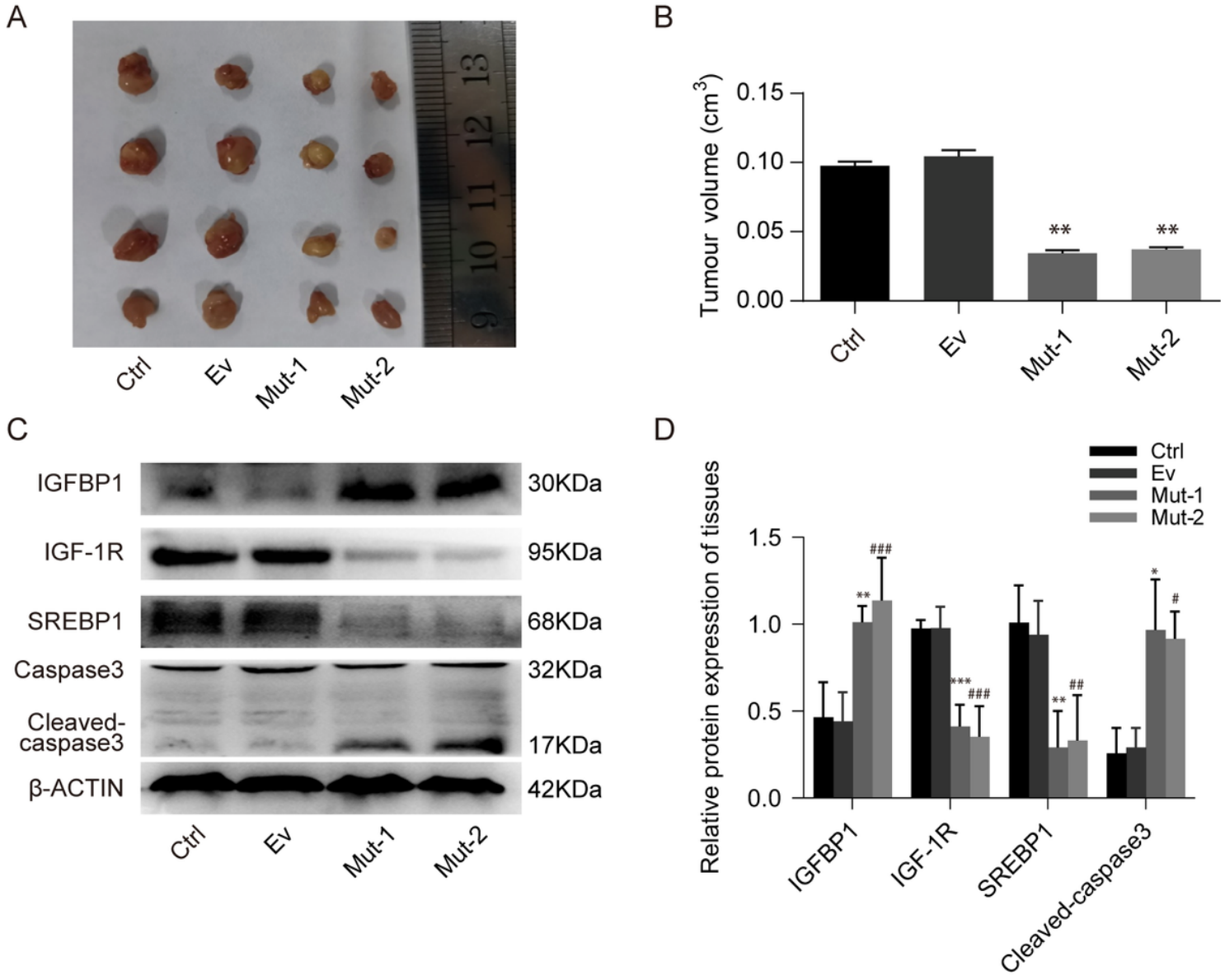

Figure 3

Effect of H3R117 MARylation on the expression of IGFBP1, IGF-1R, SREBP1, and Caspase3 in the transplanted tumor. Comparison of subcutaneously transplanted tumor in nude mice of each group (A);

the volume statistical chart of subcutaneously transplanted tumor (B); the protein expression of subcutaneously transplanted tumor in different groups (C); Statistical chart of different protein expression in the subcutaneously transplanted tumor (D) (**p < 0.01 vs. Ctrl and Ev).

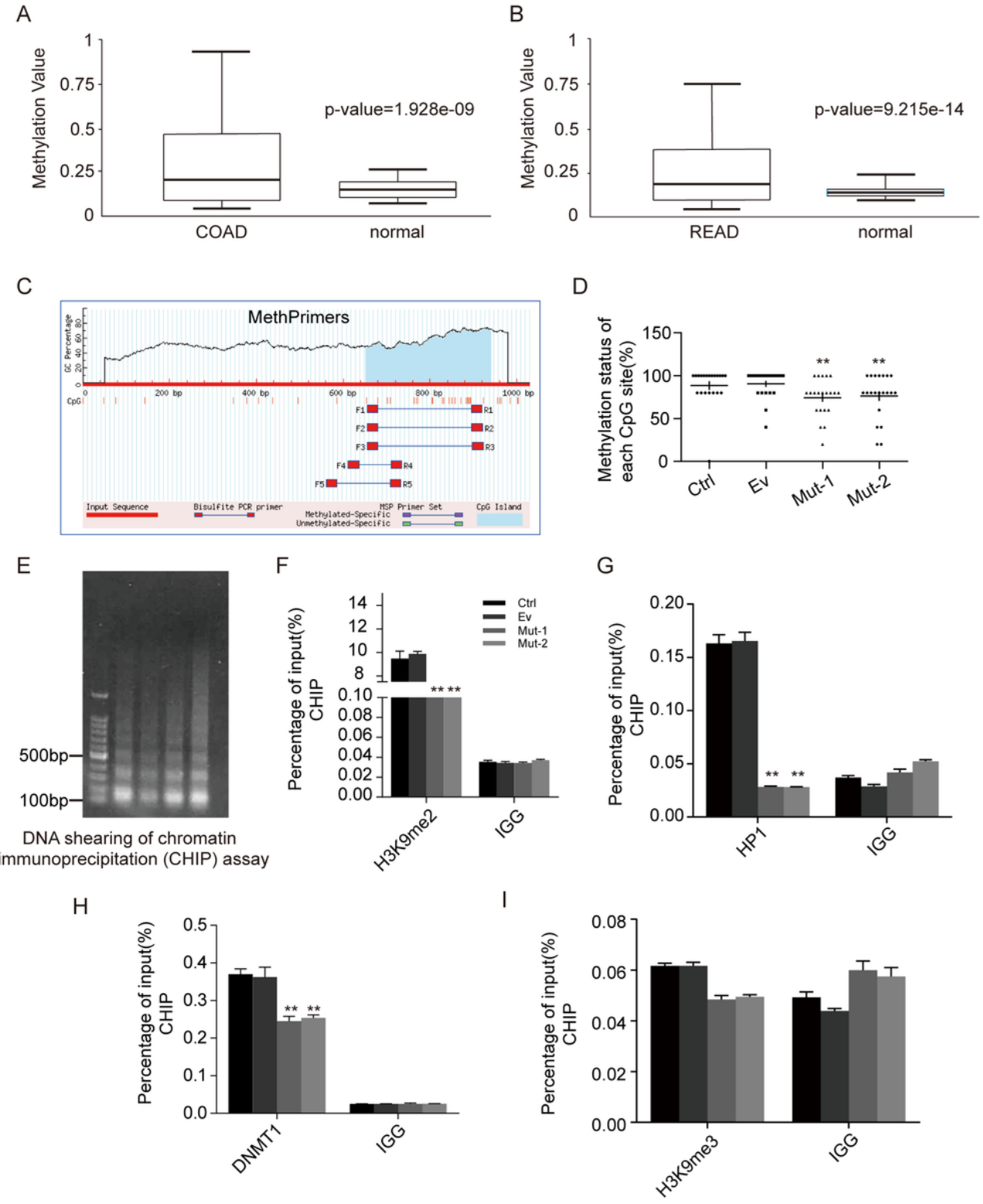

Figure 4

Effect of H3R117 MARylation on methylation of IGFBP1 promoter. (A-B) Bioinformatics analyses for the methylation of IGFBP1 promoter in COAD (A), READ, (B) and normal tissues. **(C-D)** The effect of H3R117 MARylation on the methylation of IGFBP1 promoter in LoVo cells. The CpG Island region of IGFBP1 promoter (C); methylation of the IGFBP1 promoter in different groups (D). **(E-I)** Chromatin immunoprecipitation for IGFBP1 promoter. The results of chromatin fragmentation (150–1000 bp) (E); the level of H3K9me2 on the IGFBP1 promoter (F); enrichment of HP1 on IGFBP1 promoter (G); enrichment of DNMT1 on the IGFBP1 promoter (H); the level of H3K9me3 on the IGFBP1 promoter (I). (READ, rectal adenocarcinoma; COAD, colon adenocarcinoma; **p < 0.01 vs. Ctrl and Ev)

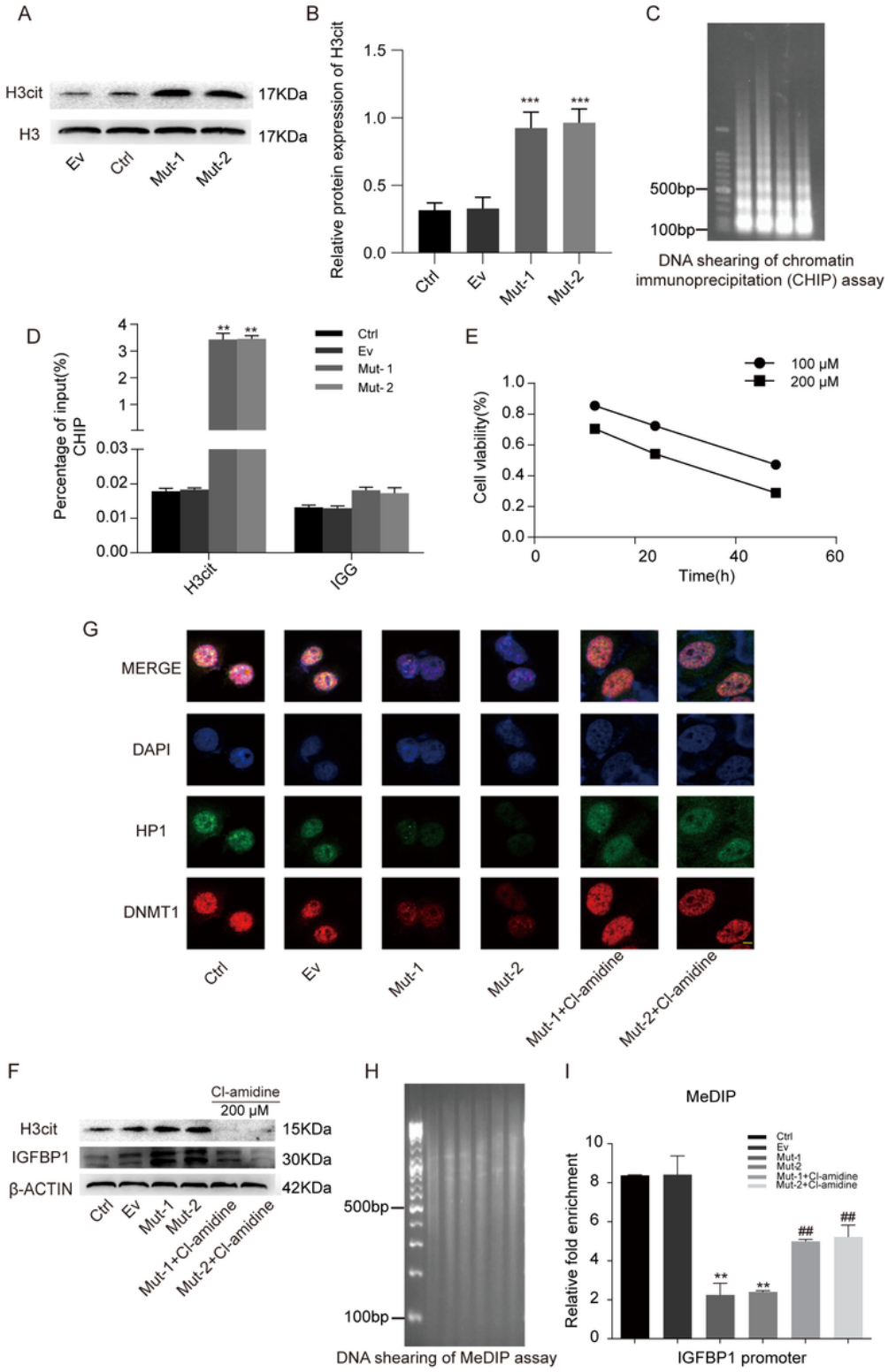

Figure 5

Effect of H3R117 MARylation on the methylation of IGFBP1 promoter by regulating H3 citrullination. (A-F) The effect of H3R117 MARylation on the IGFBP1 expression by H3 citrullination in LoVo cells. The protein expression of H3cit in different groups (A); Statistical chart of the H3cit protein expression (B) The results of chromatin fragmentation (150–1000 bp) (C); ChIP for the level of H3cit on the IGFBP1 promoter (D); the concentration and time of Cl-amidine screened by CCK-8 (E); effects of Cl-amidine on the protein

expression of H3cit and IGFBP1 (F). **(G-I)** The effect of inhibitor Cl-amidine on the co-localization of HP1 and DNMT1 and the methylation of IGFBP1 promoter. Immunofluorescent confocal microscopy for the co-localization of HP1 with DNMT1 in different groups (G). The results of chromatin fragmentation for MeDIP (H); the methylation of IGFBP1 promoter after the addition of Cl-amidine (I). (**p < 0.01 vs. Ctrl and Ev, ##p < 0.05 vs. Mut-1 and Mut-2 groups)

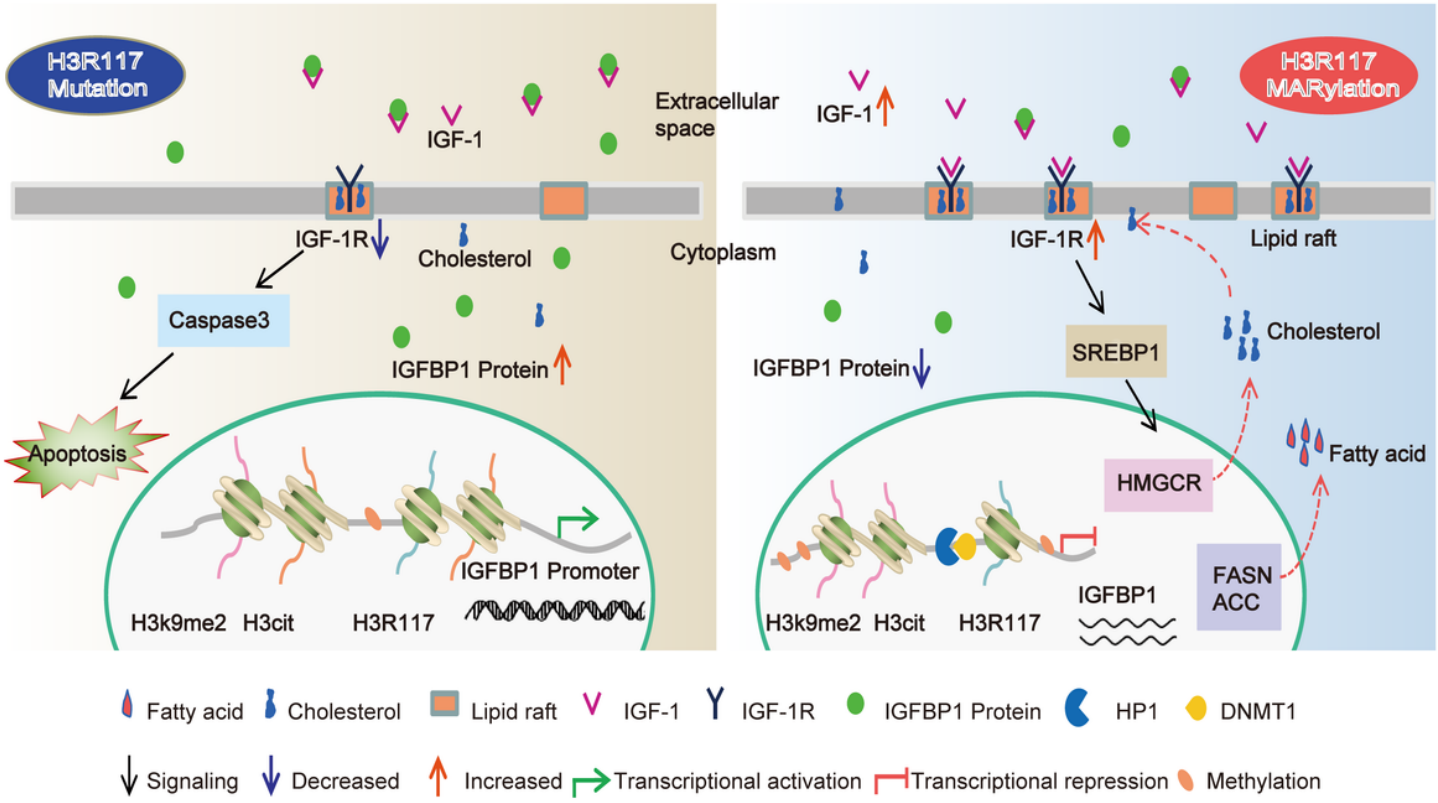

Figure 6

Illustration of the effect of H3R117 MARylation on lipid metabolism and apoptosis in CRC by regulating IGFBP1 methylation. H3R117 MARylation promotes the synthesis of fatty acids and cholesterol through IGFBP1, which promotes the binding of IGF-1 and IGF-1R, increases the expression of SREBP1 and lipid metabolism-related genes, thereby promoting the synthesis of cholesterol and IGF-1R expression of LR, thereby inhibiting apoptosis; In addition, H3R117 MARylation enhances IGFBP1 promoter methylation by inhibiting the level of H3cit, which may be one of the reasons for the decrease of IGFBP1 expression.

Supplementary Files

This is a list of supplementary files associated with this preprint. Click to download.

- SupplementaryFigure.1.tif
- SupplementaryFigure.2.tif